2026 SCEC Annual Report

Determination and Validation of Basin Structure in the San Francisco Community Velocity Model (SFCVM)

Report for SCEC Award 25296

PIs: Dr. Fan-Chi Lin
Department of Geology and Geophysics,
University of Utah, 115 S. 1460 E. Rm. 205,
Salt Lake City, UT 84112-0111

Dr. Kim B. Olsen
Department of Earth and Environmental Sciences,
San Diego State University, San Diego, CA
92182-1020

Publications and Reports: None

Summary. We have inverted period-dependent 2-10 s Rayleigh-wave horizontal-to-vertical (H/V) ratios observed for upper-crustal 1D Vs models at 149 sites across the San Francisco Bay Area. We then used the site-specific 1D Vs profiles to generate depth-dependent velocity perturbations relative to the San Francisco Velocity Model (SFVM) and a revised version of the SFVM using inverse-distance interpolation. The magnitude of the fractional change of Vs is strongest within the top 2 km, with significant Vs reduction in the immediate surrounding of the San Francisco Bay and down to roughly 3 km depth near San Jose and Santa Cruz. The revised SFCVM reduces our goodness-of-fit measure by about 7%, with the most significant improvements concentrated around the San Francisco Bay and the Santa Clara Valley. Our results show promise for improving 3D velocity models from 1D Vs profiles.

1D inversions. We have inverted for upper-crustal 1D velocity models using period-dependent Rayleigh-wave horizontal-to-vertical (H/V) ratios observed across the San Francisco Bay Area (Figure 1a). These measurements are derived from a separate SCEC project (#25266), which used multi-component noise cross-correlations from stations in Northern California (NP, NC, and BK networks) to extract Rayleigh-wave signals in the 2–10 s period range (Lin et al., 2014). Compared to surface-wave dispersion curves, Rayleigh-wave H/V ratios are particularly sensitive to velocity contrasts in the upper crust (Berg et al., 2018; Kim et al., 2025; Gkogkas et al., 2026), making them well suited for constraining shallow crustal structures relevant to earthquake ground-motion simulations. Rayleigh-wave H/V ratios at a 4 s period across the Bay Area are summarized in **Figure 1a**. Elevated H/V ratios are observed in the Oakland and San Jose regions, particularly adjacent to the South Bay, consistent with the presence of shallow, low-velocity Quaternary sediments in these areas.

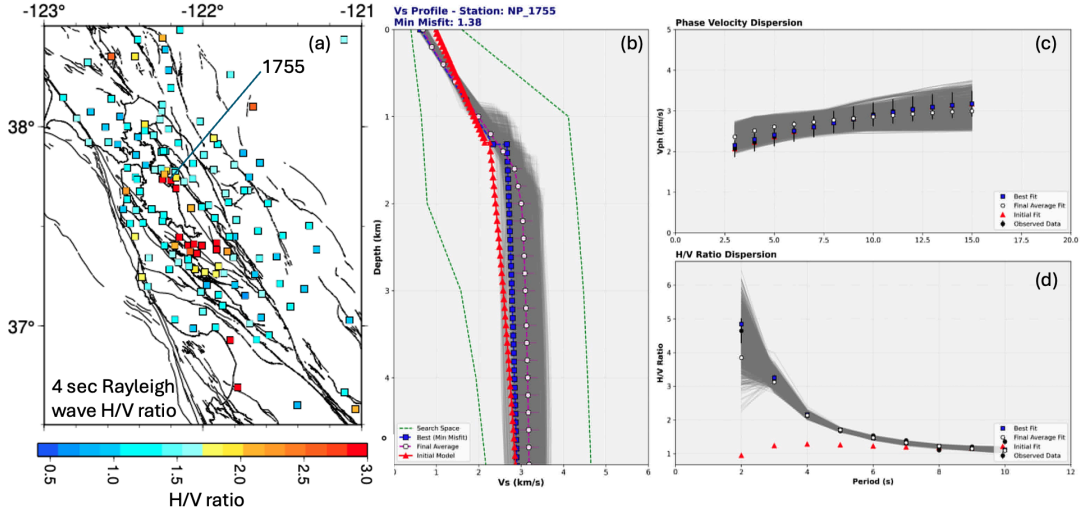

Figure 1. (a) Rayleigh-wave H/V ratios at 4 s period across the Bay Area. Station 1755, used for the 1D MCMC inversion example in (b–d), is indicated. (b) 1D Vs models at station 1755; red, gray, blue, and white curves represent the initial, acceptable, best-fit, and final (average) models, respectively. (c) Input and predicted phase velocities. (d) Observed and predicted Rayleigh-wave H/V ratios. Colors in (c) and (d) correspond to those in (b).

To stabilize the inversion, we incorporate a priori Rayleigh-wave phase velocities in the 2.5–15 s period range. These phase velocities are forward calculated from the 3D tomographic model of

Guo et al. (2025), which was constructed through a joint inversion of regional body-wave and surface-wave travel-time measurements across the Bay Area. Including these phase velocities helps anchor the deeper crustal structure of our models to the regional 3D velocity model, allowing the shallow crust to be better constrained by the H/V ratios. We adopt a 1D MCMC Bayesian joint inversion approach to simultaneously invert Rayleigh-wave phase velocities and H/V ratios (Berg et al., 2018; Kim et al., 2025). For each station, the initial 1D model is extracted from the 3D model of Guo et al. (2025).

Figure 1b–d shows an example inversion for station 1755 (NP network) near Oakland. Significant discrepancies are observed between the measured H/V ratios and those predicted by the initial 1D model. In particular, the lower predicted H/V ratios at periods below 6 s suggest that the initial model underestimates the velocity gradient in the shallow upper crust. This is not uncommon for travel-time-based tomography, which often lacks shallow sensitivity and where regularization can smear deeper structures into shallower depths. Following the MCMC inversion, the updated model exhibits a stronger shallow velocity gradient and produces H/V ratios that better match the observations while maintaining a good fit to the phase velocities. We apply this 1D MCMC inversion to all stations with available H/V measurements across the Bay Area. Vs at depths of 0.5, 1.0, and 2.0 km derived from these models are shown in **Figure 2**.

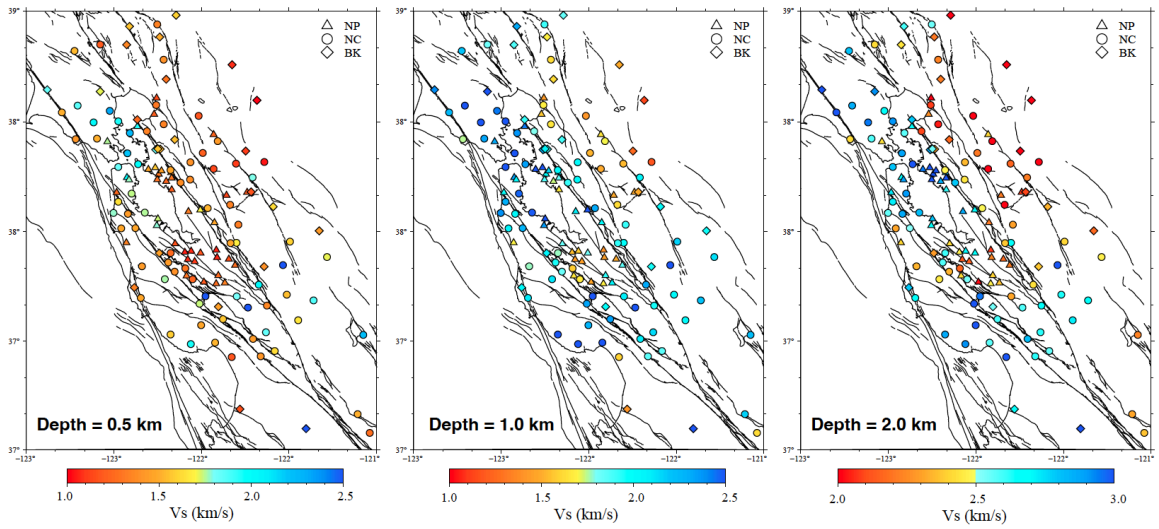

Figure 2. Inverted 1D Vs models at depths of 0.5, 1.0, and 2.0 km. Station symbols indicate the network (NP, NC, or BK).

Three-Dimensional Correction Field. To adjust the regional 3D SFVM based on the site-specific inverted 1D Vs profiles, we developed an interpolation pipeline that preserves geologically consistent trends while minimizing localized artifacts. The process begins by extracting residuals at each station, calculated as depth-averaged log-ratios, $\ln(Vs_{inv}/Vs_{SFVM})$. To stabilize these ratios against sharp velocity gradients inherent in the shallow layers of the reference model, we utilize a 250 m vertical buffer during extraction. This ensures the correction captures regional trends rather than localized noise. The maximum depth of the analysis is set to 10 km, consistent with the vertical resolution of the inversion data.

These 1D residuals are mapped into a 3D volume using a tapered inverse-distance weighted (IDW) interpolation (decay exponent of 3, maximum radius of 0.15 degrees). We then apply horizontal and vertical Gaussian filters (0.15 degrees horizontally and 500 m vertically) to ensure spatial continuity for numerical wave propagation simulations. This effectively blends inversion updates into a seamless 3D field while eliminating unphysical small-scale fluctuations. A cosine taper was applied within a depth of 8 - 10 km, gradually fading the corrections with depth to match the background SFVM. The derived 3D logarithmic ratio field was converted back to raw ratios for easy application.

The resulting adjustments of the 3D correction field (**Figure 3**) that are geologically consistent with regions inside SFVM. As anticipated, the magnitude of the fractional change is strongest within the top 2 km, capturing the high heterogeneity of shallow crustal and sedimentary layers. Prominently, the immediate surrounding of the San Francisco Bay exhibits significant Vs reduction (red patches in **Figure 3**), suggesting overestimated Vs in the SFVM for this region. The slices also highlight persisting downward revision (up to 20% reduction) near San Jose and Santa Cruz that extend down to roughly 3 km depth. Conversely, distinct shallow high-velocity patches (blue) east of the Bay fade rapidly by 2 km.

The final adjustment was then applied to the Vs values of the SFVM (**Figure 4**), where Vp and density are recalculated using standard empirical relations (Brocher, 2005) to ensure a self-consistent geophysical volume ready for validation. As can be seen, the smooth 3D correction function successfully adjusted the first-order uniformities of the original rule-based SFVM (**Figures 4a-c**) into more localized, data-driven heterogeneity (**Figures 4d-f**) while reasonably preserving the large-scale geologic framework that SFVM was based on.

Validation Simulations. To examine how the adjustment from the 3D correction field affects the accuracy of ground motion predictions, we performed numerical wave propagation simulations up to 1 Hz for seven earthquakes (M_w4.2-4.8) using the staggered-grid finite-difference code AWP-ODC (Olsen, 1994; Cui et al., 2013; Nie et al., 2017; O'Reilly et al., 2021). We conducted a comparative analysis between the SFVM with and without corrections to quantify performance gains. Following Yeh et al. (2026), the goodness-of-fit was evaluated by calculating absolute logarithmic ratios of Fourier amplitude spectra and smoothed waveform envelopes across all three components. These metrics were combined into a weighted mean error (ξ), with the regional error distribution for the model with and without corrections shown in **Figure 5a** and **5b**, respectively.

The simulation results indicate a measurable improvement in overall model performance, with the mean regional error decreasing from 0.29 to 0.27. **Figure 5c** maps the "fitness change" (ξ_{before}-ξ_{after}), where red regions indicate areas of improved model accuracy. Notably, the most significant improvements are concentrated around the San Francisco Bay and the Santa Clara Valley. **Figure 6** shows the effect of the corrections at a site in the East Bay, featuring better prediction of both amplitudes and extended coda wave energy. In summary, our validation results suggest that the proposed correction method provides a path to improving the SFVM, offering an alternative to simply re-adjusting the underlying empirical equations.

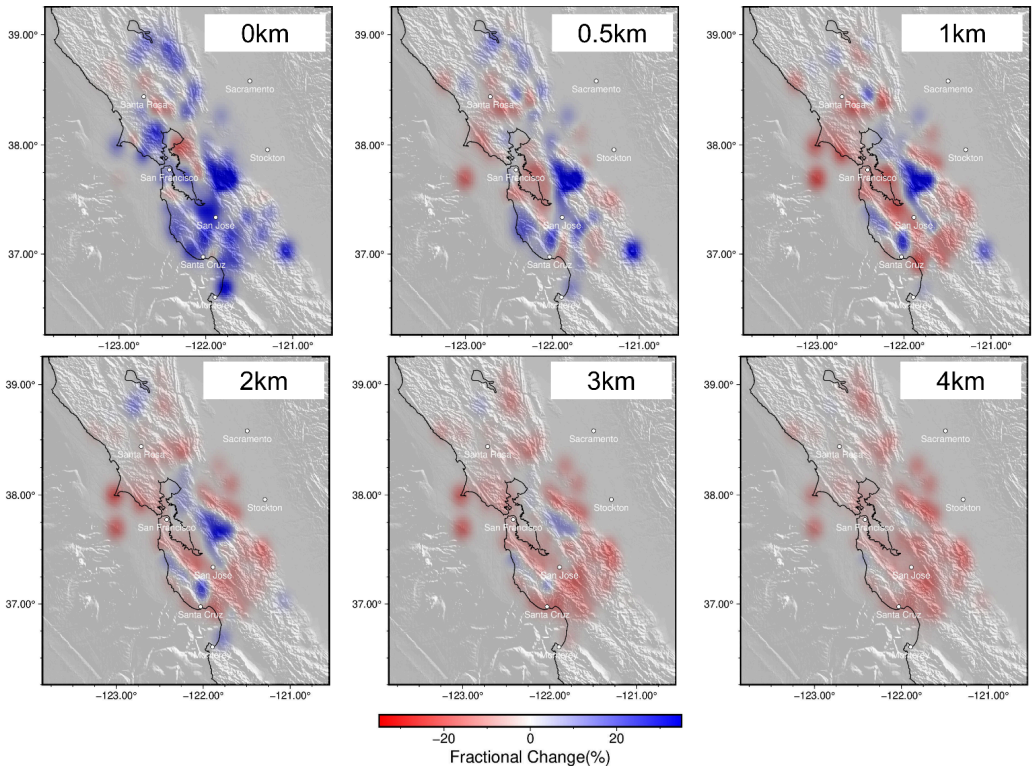

Figure 3. Horizontal slices from 0-4 km depth showing the interpolated smoothed percentage fractional change between the inverted shear-wave velocities (Vs_{inv}) and the reference model (Vs_{SFVM}), where this 3D correction field was generated using inverse-distance weighted (IDW) interpolation of depth-averaged log-ratios (defined as $\ln(Vs_{inv}/Vs_{SFVM})$).

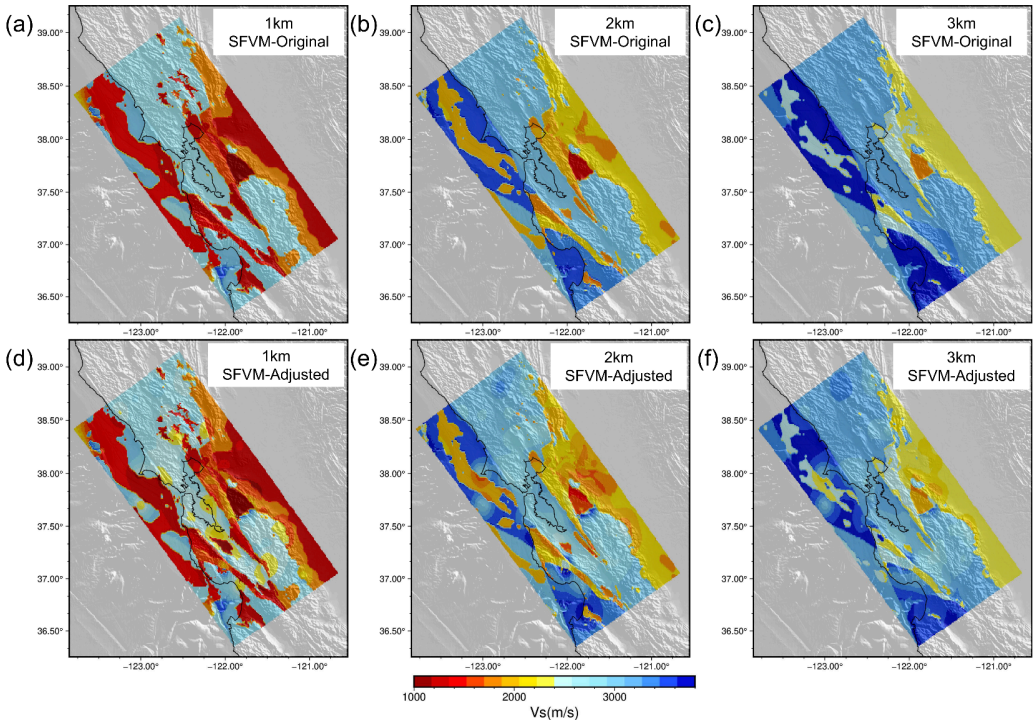

Figure 4. Comparison of horizontal Vs slices at 1 - 3 km depths of the (a-c) reference and (d-f) adjusted versions of the SFVM.

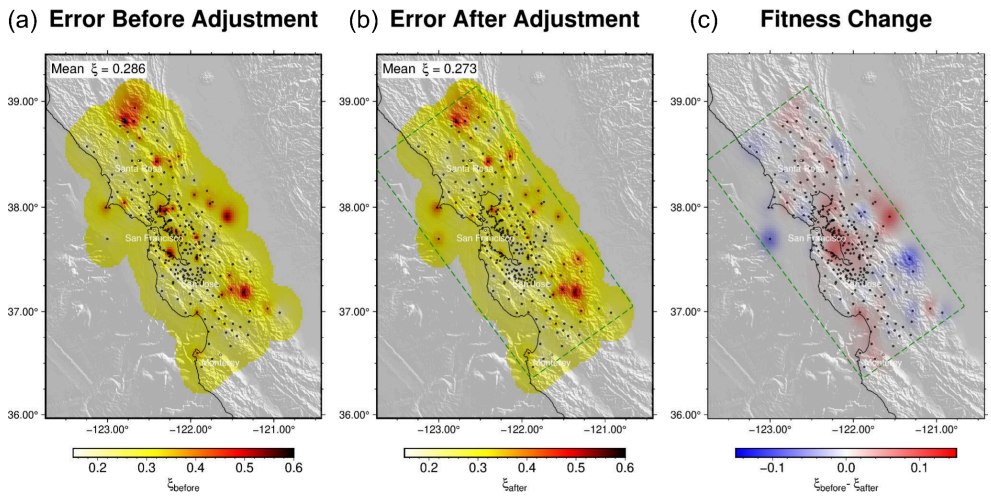

Figure 5. Comparison of model error (a) before and (b) after the adjustment shown in **Figure 1**, and (c) the difference of the two ('fitness' change, defined as ξ_{before}-ξ_{after}). Mean error value across all stations is labeled in the upper left corner of the left two panels. Increased 'fitness' to data (red) indicates improvement whereas the blue color shows worsened fit.

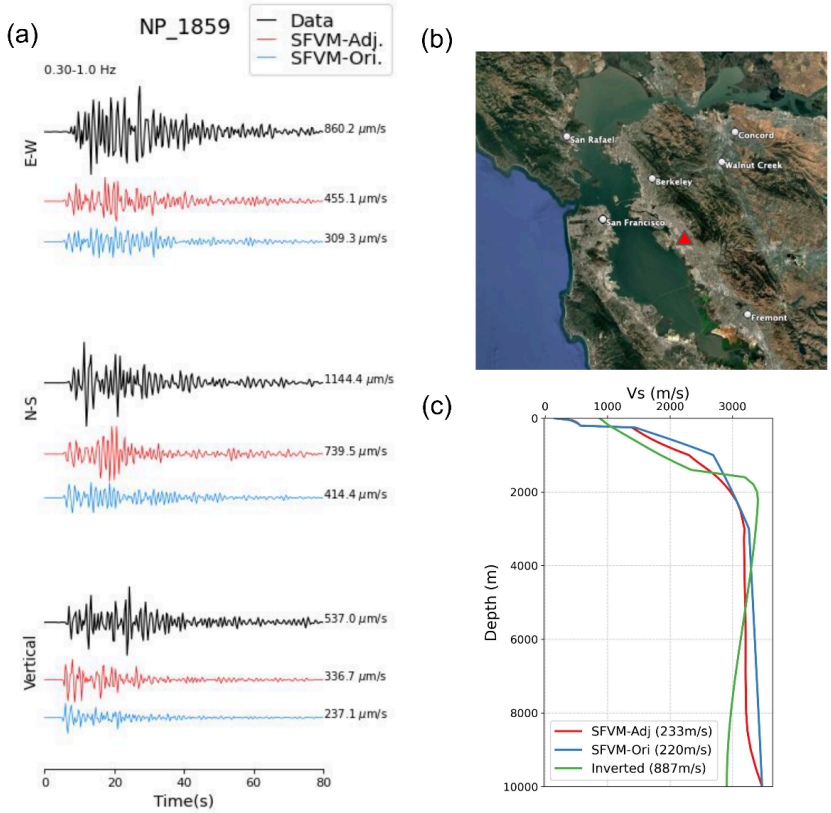

Figure 6. (a) Comparison of the 0.3 - 1 Hz synthetic velocity waveforms computed for the (red) reference and (blue) adjusted SFVM against (black) the observed waveforms at station NP.1859, located in the central East Bay (red triangle shown in panel b). The 1D Vs profile of the reference and adjusted SFVM at this station are compared with the inverted profile in (c), highlighting the lowering of Vs in the top 2 km obtained from the inversion.

References

Berg, E. M., F.-C. Lin, A. Allam, H. Qiu, W. Shen, and Y. Ben-Zion, 2018, Tomography of Southern California Via Bayesian Joint Inversion of Rayleigh Wave Ellipticity and Phase Velocity From Ambient Noise Cross-Correlations, J. Geophys. Res. Solid Earth, 123, no. 11, 9933–9949, doi: 10.1029/2018JB016269.

Brocher, T. M., 2005, Empirical Relations between Elastic Wavespeeds and Density in the Earth's Crust, Bull. Seismol. Soc. Am. 95, no. 6, 2081–2092, doi: 10.1785/0120050077.

Cui, Y., E. Poyraz, K. B. Olsen, J. Zhou, K. Withers, S. Callaghan, J. Larkin, C. Guest, D. Choi, A. Chourasia, *et al.*, 2013, Physics-based seismic hazard analysis on petascale heterogeneous supercomputers, 1–12.

Gkogkas, K., F. Lin, and R. W. Clayton, 2026, Rayleigh Wave Ellipticity and Off-Great-Circle Propagation Across the Los Angeles Basin via Dense Seismic Surveying, Seismol. Res. Lett., doi: 10.1785/0220250268.

Guo, H., T. Taira, A. Nayak, C. Thurber, and E. Hirakawa, 2025, Three-Dimensional Seismic Velocity Models for the San Francisco Bay Region, California From Joint Body-Wave and Surface-Wave Tomography Validated by Waveform Simulation, J. Geophys. Res. Solid Earth, 130, no. 6, e2025JB031377, doi: 10.1029/2025JB031377.

Kim, H., F.-C. Lin, J. C. Pechmann, C. L. Hardwick, and A. P. McKean, 2025, Seismic Imaging of the Salt Lake Basin Using Joint Inversion of Receiver Functions and Rayleigh Wave Data, J. Geophys. Res. Solid Earth, 130, no. 3, e2024JB030927, doi: 10.1029/2024JB030927.

Lin, F.-C., V. C. Tsai, and B. Schmandt, 2014, 3-D crustal structure of the western United States: application of Rayleigh-wave ellipticity extracted from noise cross-correlations, Geophys. J. Int., 198, no. 2, 656–670, doi: 10.1093/gji/ggu160.

Nie, S., Y. Wang, K. B. Olsen, and S. M. Day, 2017, Fourth-Order Staggered-Grid Finite-Difference Seismic Wavefield Estimation Using a Discontinuous Mesh Interface (WEDMI)Fourth-Order Staggered-Grid Finite-Difference Seismic WEDMI, Bull. Seismol. Soc. Am. 107, no. 5, 2183–2193, doi: 10.1785/0120170077.

Olsen, K. B., 1994, Simulation of three-dimensional wave propagation in the Salt Lake Basin, PhD Thesis, University of Utah, Salt Lake City, Utah, 157 p.

O'Reilly, O., T. Yeh, K. B. Olsen, Z. Hu, A. Breuer, D. Roten, and C. A. Goulet, 2021, A High-Order Finite-Difference Method on Staggered Curvilinear Grids for Seismic Wave Propagation Applications with Topography, Bull. Seismol. Soc. Am. 112, no. 1, 3–22, doi: 10.1785/0120210096.

Yeh, T.-Y., Y. Ben-Zion, and K. Olsen, 2026, Multi-Scale P and S Seismic Velocity Models of California and Western Nevada, ESSOAr., https://doi.org/10.22541/essoar.15001929/v1.